International Journal of Research (IJR)
e-ISSN: 2348-6848, p- ISSN: 2348-795X Volume 2, Issue 10, October 2015
Available at http://internationaljournalofresearch.org

Power Quality Improvement of Switched Reluctance Motor Drives

Pattan Fazil
M-tech Student Scholar Department of EEE, Guntur Engineering College, Guntur (Dt); A.P, India.
Fazileee09@gmail.com
P.Suman Pramodkumar
M.Tech Associate Professor Department of EEE, Guntur Engineering College, Guntur (Dt); A.P, India.
Sumanprmd@gmail.com

Abstract-
The Switched Reluctance Motor (SRM) drive has evolved as an alternative to conventional motors in variable speed drives because of advantages like simple and rugged structure, absence of rotor winding, adaptability to harsh environments and high speed operation. An observer is introduced to guarantee both fast response and stability of the dead-beat current controller. The controller is tested for two different speeds at three different load torques. Steady state analysis of the drive has been carried out. The proposed digital PWM current controller has almost the same performance as hysteresis current regulation and at the same time, avoids its drawbacks. Variable switching frequency in hysteresis control makes it difficult to design the electromagnetic interference (EMI) filter and may cause acoustical noise. Even though the analog-to-digital converters (ADC) nowadays could have very high sampling rates, EMI caused by the converter would add great noise to the sampling process, which might cause fault in the operation of SRM. Current control is essential in SRM drives. Conventionally, hysteresis current regulation is utilized for current control in SRM drives, but it has some drawbacks including high sampling rate requirement, sensitivity to switching EMI noise, and varying switching frequency. In order to design a current controller with both fast dynamic response and small tracking error, more information of model of SRM is needed. With its flux linkage profile, an SRM could be well modeled and simulated by using MAT Lab/Simulink.

Index Terms— Power quality; Power factor correction (PFC); SRM; Mid-point converter.

I. INTRODUCTION

In the recent few years , Switched Reluctance Motor (SRM) have attracted renewed interest and become a competitive selection for many application of electric drive system due to its relative simple construction, reliability, fast response because of torque to inertia ratio and low cost. So with relatively simple converter and control requirement the SRM is gaining an increasing attention in drive industry. SRM uses power converter for its operation and they need a stable dc supply [1-2]. The conventional SRM drive usually includes a simple diode rectifier with a filter capacitor used as a front-end converter. Although this structure is simple but it draws a pulsating ac line current resulting in poor power quality that is low power factor and high harmonic content in the line current.

The switched reluctance motor (SRM) represents one of the earliest electric machines which was introduced two centuries back in the history. It was not widely spread in industrial applications such as the induction and dc motors due to the fact that at the time when this machine was invented, there was no simultaneous progress in the field of power electronics and semiconductor switches which are necessary to drive this kind of electrical machines properly. The problems associated with the induction and dc machines together with the revolution of power electronics and semiconductors in the late sixties of the last century led to the reinvention of this motor and redirected the researchers to pay attention to its attractive features and advantages which helped in overcoming a lot of problems associated with other kinds of electrical machines such as brushes and commutators in dc machines and slip rings in wound rotor induction machines besides the speed limitation in both these motors. The simple design and robustness of the switched reluctance machine made it an attractive alternative for these kinds of electrical machines for many applications recently specially that most of its disadvantages which are mentioned in the following chapter could be eliminated or minimized by use of high speed and high power semiconductor switches such as the power thyristors, power GTOs, power transistors, power IGBTs and the power MOSFETs. The availability and the inexpensive cost of these power switches nowadays besides the presence of microprocessors and microcontrollers, PIC controllers and DSP chips makes it a strong opponent to other types of electrical machines.

II. DEAD-BEAT CONTROLLER FOR SRM

Neglecting the mutual coupling between the phases, the phase voltage equation of SRM can be given as:

$$u = Ri + \frac{d\psi(\theta, i)}{dt} \tag{1}$$

Where u is the phase voltage, R is the winding resistance, ψ is the flux linkage, θ is the rotor position and i is the phase current. When SRM is controlled digitally, (1) should be expressed in discrete-time domain as:

$$u(k) = R\cdot i(k) + \frac{\psi(\theta(k+1), i(k+1)) - \psi(\theta(k), i(k))}{T} \tag{2}$$

Where T is the control period and k is a positive integer representing the sampling instant. In practice, the flux linkage profile ψ(θ(k), i(k)) is obtained by experimental measurement or FEA. Using the information on flux linkage, a dead-beat controller could be realized by

$$u(k) = R\cdot i(k) + \frac{\psi(\theta(k+1), i_{ref}) - \psi(\theta(k), i(k))}{T} \tag{3}$$

Where i_{ref} is the reference current. θ(k+1)=θ(k)+ω·T and ω is the angular speed. When (3) is substituted in (2), the response of system could be obtained as

$$\psi(\theta(k+1), i(k+1)) = \psi(\theta(k+1), i_{ref}) \tag{4}$$

The transfer function of (4) is given as

$$\frac{\psi}{\psi_{ref}} = 1 \tag{5}$$

Where ψ_{ref} is the reference flux calculated by rotor position θ and reference current i_{ref}. It is shown that with the information of the accurate model of SRM, dead-beat controller could track the reference within one control period.(5) also indicates the system with dead-beat controller is inherently stable.

However, the dead-beat controller relies on the accurate model of the SRM. If the model is not accurate enough, the dead-beat controller would not have its ideal performance. In practice, both the flux linkage profile and the winding resistance might not be obtained accurately, either by FEA or by experimental measurement. Especially when the SRM is massively produced, there must be inconsistence between each motor. In addition, the winding resistance would vary with temperature. In order to model the inaccuracy of the flux linkage profile and the phase resistance, the following expressions are used:

$$\psi_m = \alpha\cdot\psi$$
$$R_m = \gamma\cdot R \tag{6}$$

where ψ_m is the experimentally measured or FEA based flux linkage profile, and R_m is the measured or calculated winding resistance. α represents the mismatch factor between the flux linkage profile of the model and the real flux linkage profile, whereas γ represents the mismatch between the modeled and real winding resistance. A and γ are both unknown parameters. For the reason that the flux linkage profile and winding resistance are obtained by FEA or experimental measurements, the mismatch factors are not going to be too large. Therefore, α and γ are assumed to be around 1 with boundaries: $\alpha_{min}<\alpha<\alpha_{max}$, $\gamma_{min}<\gamma<\gamma$ max. In this case the dead-beat controller in (3) could be redesigned as:

$$u(k) = R_m\cdot i(k) + \beta\frac{\psi_m(\theta(k+1), i_{ref}) - (\psi_m\theta(k), i(k))}{T} \tag{7}$$

Where β is the gain of the controller. After substituting (7) in (2), the response of the system could be obtained as:

$$\begin{aligned}&\psi(\theta(k+1), i(k+1))\\&= (1-\alpha\cdot\beta)\psi(\theta(k), i(k)) + \alpha\cdot\beta\cdot\psi(\theta(k+1), i_{ref})\\&-(1-\gamma)R\cdot i(k)\cdot T\end{aligned} \tag{8}$$

For a high enough sampling frequency, sampling period T can be considered small enough. In order to facilitate the stability analysis, the term (1−γ)R·i(k)·T is neglected. The transfer function of the system is given as:

$$\frac{\psi}{\psi_{ref}} = \frac{\alpha\cdot\beta z}{z-(1-\alpha\cdot\beta)} \tag{9}$$

According to (9), the system with controller of (7) is stable only when α·β satisfies

$$0<\alpha\cdot\beta<2 \tag{10}$$

International Journal of Research (IJR)
e-ISSN: 2348-6848, p- ISSN: 2348-795X Volume 2, Issue 10, October 2015
Available at http://internationaljournalofresearch.org

Equation (10) indicates the maximum mismatch between model and real parameter, and β should be properly selected to guarantee the stability of the controller. If $\alpha \cdot \beta = 1$, Equation (9) becomes (5), which is the most stable case.

III. GAIN OBSERVER DESIGN FOR DEAD-BEAT CONTROLLER

The mismatch factor α actually varies with different motors. After figuring out the boundaries of α, it is only possible to select the controller gain β to make sure the controller is stable, while it is not possible to find a single β which guarantees the controller to work with ideal performance for all motors. In this case, an observer should be developed to adapt the gain β for different motors. Let

$$e_1 = \psi_m\left(\theta(k), i_{ref}\right) - \psi_m\left(\theta(k), i(k)\right)$$
$$e_2 = \psi_m\left(\theta(k), i_{ref}\right) - \psi_m\left(\theta(k-1), i(k-1)\right) \quad (11)$$

According to (8), there is

$$e_1 - \frac{(1-\gamma)}{\gamma}\alpha \cdot R_m \cdot i(k-1) \cdot T = (1-\alpha \cdot \beta) e_2 \quad (12)$$

According to (12), if $\alpha \cdot \beta < 1$, then the left part should have the same sign as the right part. If $\alpha \cdot \beta > 1$, the left part should have different sign as the right part. It is indicated that if the left part and the right part have the same sign, $\alpha \cdot \beta$ is less than 1. Therefore, the controller gain β should be increased to make $\alpha \cdot \beta = 1$. If the left part and the right part have different signs, then it is indicated that $\alpha \cdot \beta$ is greater than 1. In this case, the controller gain β should be decreased to make $\alpha \cdot \beta = 1$.

However, in (12), the values of α and γ are not known. With the boundaries of α and γ, there is.

$$-B_{\alpha\gamma} < \frac{(1-\gamma)}{\gamma}\alpha < B_{\alpha\gamma} \quad (13)$$

Assuming that $B = B_{\alpha\gamma} R_m |i(k-1) T|$, then the idea of the gain regulator could be shown in Fig. 1. If e1is located in area I or II, and then the controller gain β should be adjusted according to the signs of e1and e2. If e1is located within the area between Band-B, the controller gain should be kept the same because due to the uncertainty of α and γ, the sign of e1is unknown.

According to the idea above, the gain observer could be designed as

$$\beta(k+1) = \beta(k) + \Delta\beta(k)$$
$$\Delta\beta(k) = \begin{cases} |K_1|, e_1 \cdot e_2 > 0 \ and \ |e_1| > B \\ 0, |e_1| \le B \\ -|K_2|, e_1 \cdot e_2 < 0 \ and \ |e_1| > B \end{cases} \quad (14)$$

Where $K_1$and $K_2$are the gains of the gain observer. According to (8), the error transfer function of the system is

$$e(k+1) = (1-\alpha\beta(k))\Delta\psi_{ref}(k) + O(k) + (1-\alpha\beta(k))e(k) \quad (15)$$

Where

$$\Delta\psi_{ref}(k) = \psi_m\left(\theta(k+1), i_{ref}\right) - \psi_m\left(\theta(k), i_{ref}\right)$$
$$O(k) = \frac{(1-\gamma)}{\gamma}\alpha \cdot R_m \cdot i(k) \cdot T \quad (16)$$

To analysis the stability of the system and figure out the boundaries of $K_1$and K_2, a Lyapunov function is considered as

$$V(k) = \left(e'(k)\right)^2$$
$$e'(k) = \Delta\psi_{ref}(k) + e(k) \quad (17)$$

Then, the increase of the Lyapunov function is

$$\Delta V(k) = V(k+1) - V(k)$$
$$= \left[\Delta\psi_{ref}(k+1) + O(k) - \alpha \cdot \beta(k) V(k)\right]$$
$$\cdot \left[\Delta\psi_{ref}(k+1) + O(k) + (2 - \alpha \cdot \beta(k)) V(k)\right] \quad (18)$$

It is shown that (18) is a parabola. The direction of the parabola is defined by $-\alpha \cdot \beta(k)(2-\alpha \cdot \beta(k))$. If α and β(k) satisfy (10), the parabola goes downwards with two roots as shown in Fig. 2. The two root of (18) are

$$v_1 = -\frac{\Delta\psi_{ref}(k+1) + O(k)}{2 - \alpha \cdot \beta(k)}$$
$$v_2 = \frac{\Delta\psi_{ref}(k+1) + O(k)}{\alpha \cdot \beta(k)} \quad (19)$$

It is shown in Fig. 2 that if α and β(k) satisfy (10), no matter what the initial value of V(k) is, it will eventually moves to and stop at $v_1$or v_2.

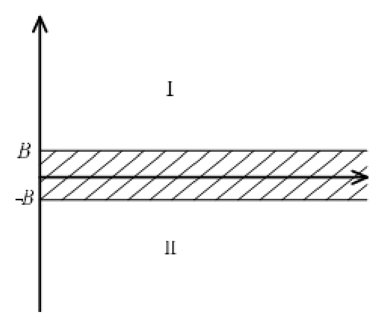

Fig.1 Effective area of gain observer.

International Journal of Research (IJR)
e-ISSN: 2348-6848, p- ISSN: 2348-795X Volume 2, Issue 10, October 2015
Available at http://internationaljournalofresearch.org

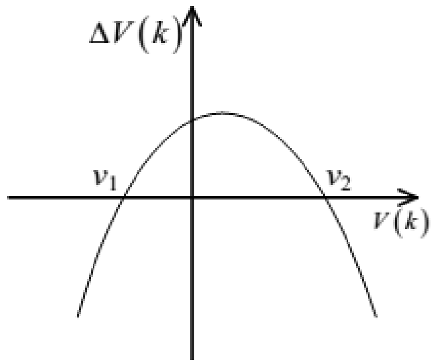

Fig.2. the shape of (18)

(19) Defines the steady state error caused by the change of control reference and by the mismatch of winding resistance. For the reason that the sample frequency is high enough (10 kHz), both $\Delta\psi_{ref}$ (k) and O (k) are small enough. It means even though this controller could have dynamic and steady state errors, but they are both small enough and are also bounded.

According to (14) and (15), if $0<\alpha\cdot\beta(k)<1$, V(k) is going to move to $v_1$or v_2 along one side of the parabola. This means β (k) is too small. In this case, β(k)is going to be increased by (14). If $1<\alpha\cdot\beta(k)<2$, V (k) is going to move to v1or v2 by jumping between the two sides of the parabola. This means β(k) is too large. In this case, β(k) is going to be decreased by (14). Therefore, the system has guaranteed stability by (14) when α and β (k) satisfy (10).

If α and β(k) don't satisfy (10), which is $\alpha\cdot\beta(k)>2$, the direction of the parabola is going to be upwards and V(k) is going to move away from v1 or v2 by jumping between the two sides of the = parabola. In this case, (14) is going to decrease β (k), which drives α·β (k) to the stable area. Therefore, (14) stabilizes the system globally.

According to (10), the boundaries of $K_1$and $K_2$are

$$0 < K_1 < 2/\alpha$$
$$0 < K_2 < \beta(k) \tag{20}$$

In practice, the phase voltage u (k) is limited by the DC bus voltage UDC. If the calculated u(k-1)exceeds UDC or −UDC, it means the controller output has reached its limits, and can't be adjusted further even the gain is increased. In this case, the observer should be disabled.

IV.CURRENT SAMPLE FOR DIGITAL CONTROL

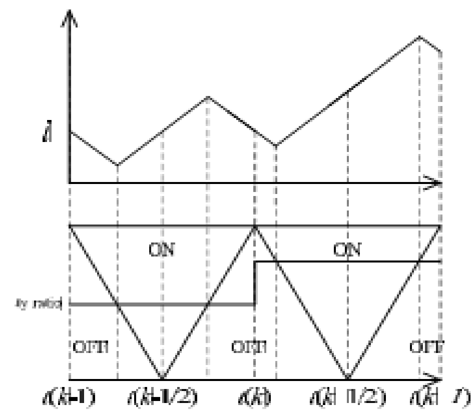

Fig.3 PWM modulation.

Fig. 3 shows the PWM modulation for digital control. In the kth control period, current should be sampled at t(k). In practice, especially in DSP control, if current is sampled at t(k), it will take some time for the controller to calculate the duty ratio and the duty ratio for t(k)is actually loaded into the PWM modulator at t(k+1). This brings a sampling time delay into the control loop.

In this case, the transfer function of the controller changes form (9) to

$$\frac{\psi}{\psi_{ref}} = \frac{\alpha\beta z}{z^2 - z + \alpha\beta} \tag{21}$$

Compared to (9), (21) reduces the maximum gain of the controller and brings oscillations. [8] Proposes a predictive current controller to solve the problem. While predictive current controller increases the calculation burden for DSP, especially for nonlinear systems such as SRMs. [7] recommends that current should be sampled at t(k−1/2), which means i(k) is estimated by

$$\hat{i}(k) = i(k-1/2) \tag{22}$$

It is shown in Fig. 3 that there is no switch action at t(k−1/2), so the EMI noise is avoided. Furthermore, this method allows DSP to process the duty ratio calculation in half period and will not bring delay to the control loop.

The estimation of (22) is accurate if the current of each control period stays the same, as the $(k-1)^{th}$ period shown in Fig.3. If current between each control period is changing, as the k^{th} period in Fig. 3, (22) is not accurate. If the current is not sampled accurately, it will bring oscillations to the control results and will reduce the performance of the controller. As shown in

Fig. 3, with the symmetrical modulation, the current waveform of the former half period and the latter half period is symmetric. Therefore, the current i(k) could be estimated by

$$\hat{i}(k) = 2i(k-1/2) - i(k-1) \tag{23}$$

(23) Demands current to be sampled at both t(k−1/2) and t(k−1), which doubles the sample rate. The ADCs used in motor control usually is capable of working at the sampling rate of twice of the PWM frequency without increasing any cost. (23), similar to (22), also avoids the EMI noise caused by the switching action, provides half control period's time to calculate the duty ratio, and will not bring delay to the control loop.

V.MATLAB/SIMULINK RESULTS

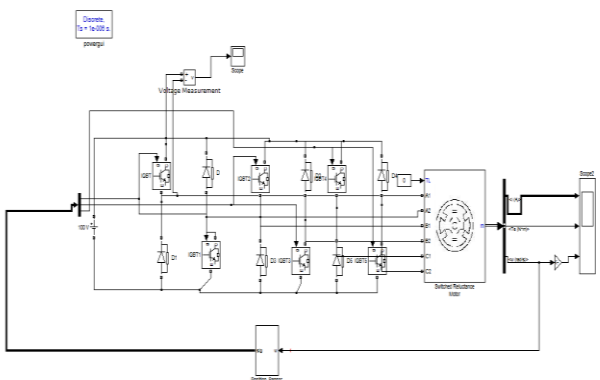

Fig.4.Matlab/Simulink Model Of Without Proposed Observer.

Fig.4. shows the Matlab/Simulink model of without proposed observer.

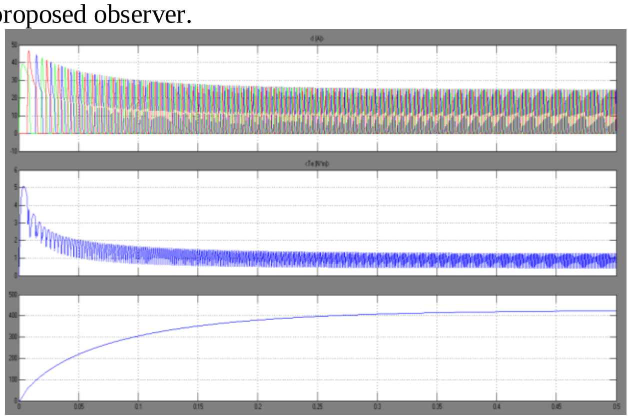

Fig.5. Simulation wave forms of current, torque speed without control.

Fig.5.shows the Simulation wave forms of current, torque speed without control.

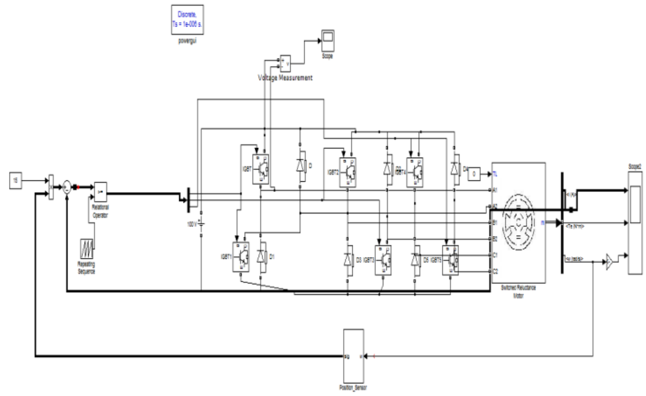

Fig.6.Matlab/Simulink Model Of With PWM Proposed Observer.

Fig.6.shows the matlab/simulink model of with PWM proposed observer.

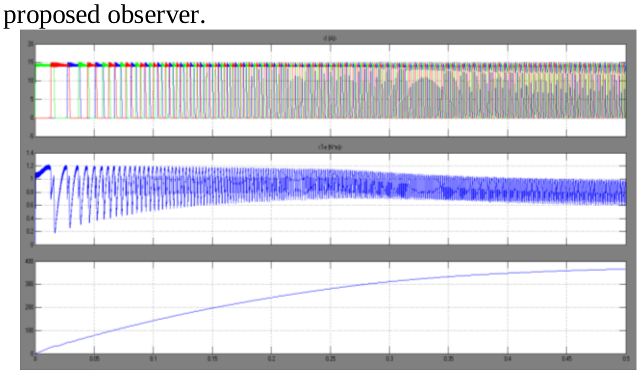

Fig.7. Simulation wave forms of current, torque speed with PWM.

Fig.7.shows the Simulation wave forms of current, torque speed with PWM.

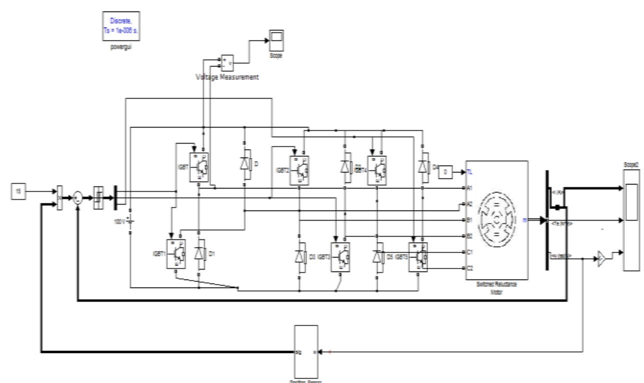

Fig.8.Matlab/Simulink Model Of With Hysteresis Control Proposed Observer.

Fig.8.shows the Matlab/Simulink Model Of With Hysteresis Control Proposed Observer

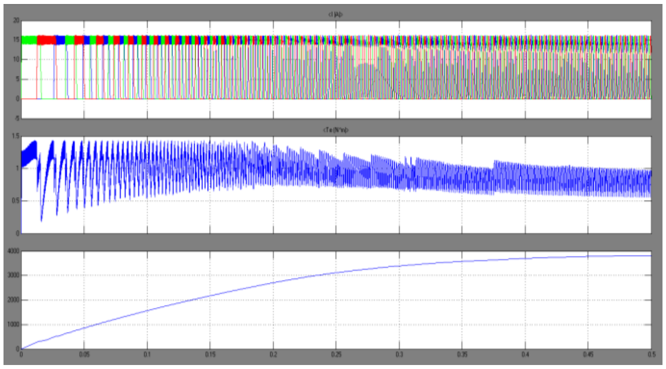

Fig.9. Simulation wave forms of current, torque speed with hysteresis control.

Fig.9. shows the Simulation wave forms of current, torque speed with hysteresis control.

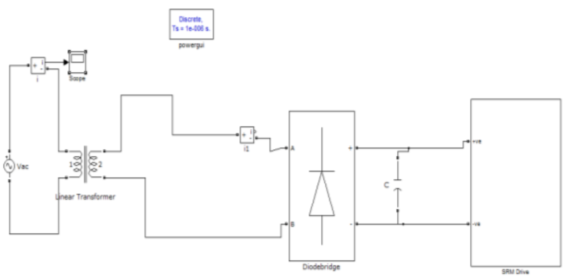

Fig.10.Matlab/Simulink Model Of Without APF and With PWM.

Fig.10.shows the Matlab/Simulink Model Of Without APF and With PWM.

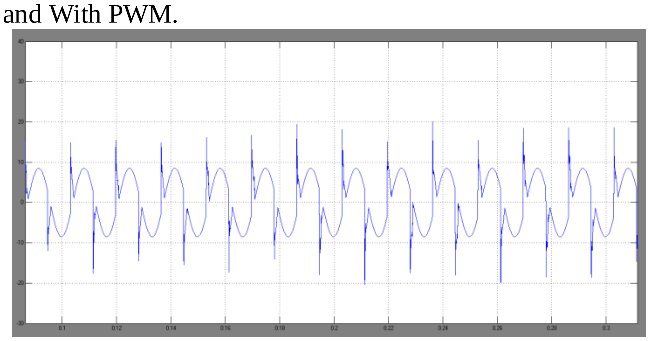

Fig.11. Source current of the without APF.

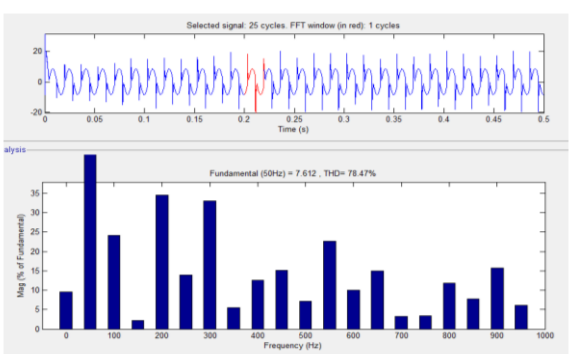

Fig.12. Total harmonics distortions for source current.

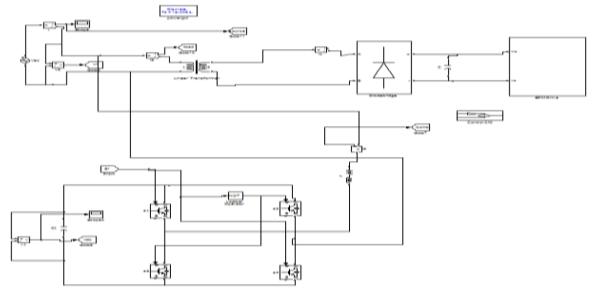

Fig.13.Matlab/simulink model of with APF and with PWM.

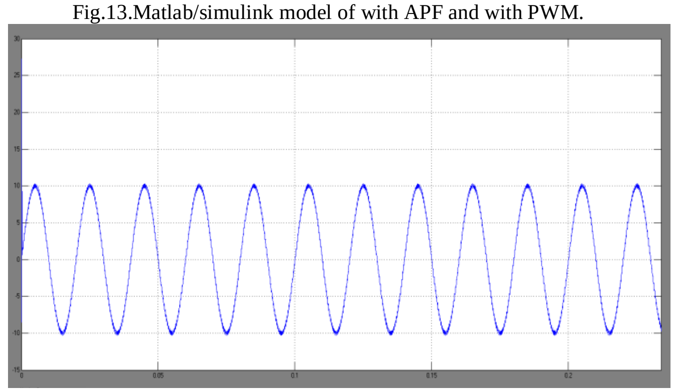

Fig.14. Source current of the with APF.

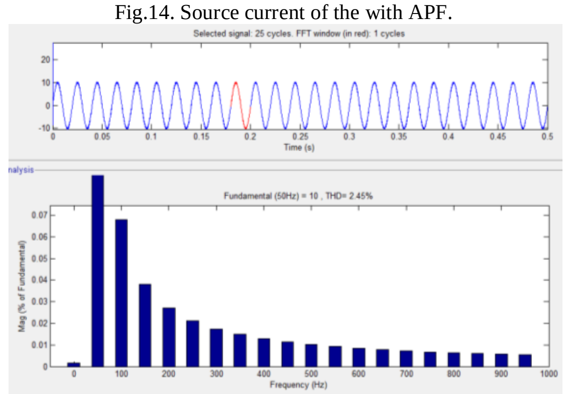

Fig.15.Total harmonics distortions for source current.

VI. CONCLUSION

This paper proposes a dead-beat current controller for SRM drives. An observer is introduced to guarantee both fast response and stability of the dead-beat current controller. An improved current sampling method is proposed to make the current sampling accurate even under varying current conditions. The voltage at the dc link capacitor are kept balanced which is needed for the stable operation of mid-point converter fed SRM drive. The performance of a switched reluctance motor drive is simulated in MATLAB/SIMULINK environment using asymmetric bridge converter where various drives parameter such as stator voltage, flux linkage, stator current, electromagnetic torque, rotor speed and position are being analyzed and discussed. Further bacterial foraging optimization technique is used to locate the best optimum position of rotor and stator where torque ripples are minimized and also THD value compare the without APF and with APF we can improve the source current THD.

REFERENCES

[1] S. Vukosavic and V.R. Stefanovic, "SRM Inverter Topologies: A Comparative evaluation", IEEE Trans. on Industry. Applications, vol.27, no. 6, pp 1034-1047, Nov/Dec. 1991.

[2] Pollock and B. W. Williams, "Power converter circuits for switched reluctance motors with the minimum number of switches," in Proc. Inst. Elect. Eng., vol. 137, pt. B, no. 6, 1990, pp. 73–384.

[3] T. J. E. Miller, Switched Reluctance Motors and Their Control. Oxford, U.K.: Clarendon: Oxford University Press, 1993.

[4] J.-W. Ahn, S.-G. Oh, and J.-W. Moon, "A three-phase switched reluctance motor with two-phase excitation," IEEE Trans. Ind. Appl., vol. 35, no. 5, pp. 1067–1075, 1999.

[5] J.-W. Ahn, S.-J. Park, and D.-H. Lee, "Hybrid excitation of SRM for reduction of vibration and acoustic noise," IEEE Trans. Ind. Electron., vol. 51, no. 2, pp. 374–380, Apr. 2004.

[6] Dong-Hee Lee; Zhen-Guo Lee; Jin-Woo Ahn, "Instantaneous Torque Control of SRM with a Logical Torque Sharing Method," Power Electronics Specialists Conference, 2007. PESC 2007. IEEE, Orlando, FL June 2007, pp. 1784–1789.

[7] H. Goto, A. Nishimiya, H.-J. Guo, and O. Ichinokura, "Instantaneous torque control using flux-based commutation and phase-torque distribution technique for SR motor EV," COMPEL Int. J. Comput. Math. Electr. Electron. Eng., vol. 29, no. 1, pp. 173–186, 2010.

[8] J. Ye, B. Bilgin, and A. Emadi, "Comparative evaluation of power converters for 6/4 and 6/10 switched reluctance machines," in Proc. 2012 IEEE Transportation Electrification Conference and Expo (ITEC), Dearborn, MI, June 2012, pp. 1–6.

[9] F. Blaabjerg, P. C. Kjaer, P. O. Rasmussen, and C. Cossar, "Improved digital current control methods in switched reluctance motor drives," IEEE Trans. Power Electron., vol. 14, no. 3, pp. 563–572, May 1999..

[10] Y. A.-R. I. Mohamed and E. F. El-Saadany, "Robust High Bandwidth Discrete-Time Predictive Current Control with Predictive Internal Model—A Unified Approach for Voltage-Source PWM Converters," IEEE Trans. Power Electron. vol. 23, no. 1, pp. 126–136, Jan. 2008.

[11] B. Shao and A. Emadi, "A digital PWM control for switched reluctance motor drives," in Proc. 2010 IEEE Vehicle Power and Propulsion Conference, Lille, France, Sept. 2010.

Pattan Fazil was born in Nizampatnam, India. He received his B.Tech Degree in Electrical and Electronics Engineering from Chebrolu Engineering College, Chebrolu, Guntur dist India. Presently, he is pursuing M.Tech (Power systems) at Guntur Engineering College, Guntur India. His current research interest includes Electrical Machines and Power system, power electronics.

P.Suman pramod kumar M.Tech presently working as Associate professor in Department of EEE, Guntur engineering college, Guntur. He has 12 years of teaching Experience in various Engineering colleges and having 15 no of International/national journals. His areas of interest are in Power system stability, Control system and Electromagnetic fields